



Supplementary Materials

Reduced Graphene Oxide Aerogels with Functionalization-Mediated Disordered Stacking for Sodium-Ion Batteries

Jaehyeung Park ^{1,2}, Jaswinder Sharma ¹, Charl J. Jafta ¹, Lilin He ³, Harry M. Meyer III ⁴, Jianlin Li ¹, Jong K. Keum ^{3,5}, Ngoc A. Nguyen ^{4,†} and Georgios Polizos ^{1,*}

¹ Electrification and Energy Infrastructures Division, Oak Ridge National Laboratory, Oak Ridge, TN 37831, USA; parkj@knu.ac.kr (J.P.); sharmajk@ornl.gov (J.S.); jaftacj@ornl.gov (C.J.J.); lij4@ornl.gov (J.L.)

² Department of Bio-Fibers and Materials Science, Kyungpook National University, Daegu 41566, Korea

³ Neutron Scattering Division, Oak Ridge National Laboratory, Oak Ridge, TN 37831, USA; hel3@ornl.gov (L.H.); keumjk@ornl.gov (J.K.K.)

⁴ Chemical Sciences Division, Oak Ridge National Laboratory, Oak Ridge, TN 37831, USA; meyerhmiii@ornl.gov (H.M.M.III); nanguyen@illinois.edu (N.A.N.)

⁵ Center for Nanophase Materials Sciences, Oak Ridge National Laboratory, Oak Ridge, TN 37831, USA; keumjk@ornl.gov (J.K.K.)

* Correspondence: polyzosg@ornl.gov

† Current address: Applied Research Institute, University of Illinois at Urbana-Champaign, 2100 S Oak St., Champaign, IL 61820, USA.

The XPS survey spectra and the surface composition of the GO platelets that were used for the hydrothermal synthesis of the aerogels as well as the XPS analysis of the rGO, rGO-CD, and rGO-EDA aerogels are shown in Figure S1. The aerogels were reduced during the hydrothermal process and the oxygen content was decreased significantly.

Oscillatory strain sweep tests were conducted from 0.1 to 20% at an angular frequency of 10 rad/s. The storage and loss modulus values in Figure S2 are in good agreement with the modulus values in Figure 3. The tested aerogels were freeze-dried, and the modulus values started to drop at oscillation strains higher than 10%.

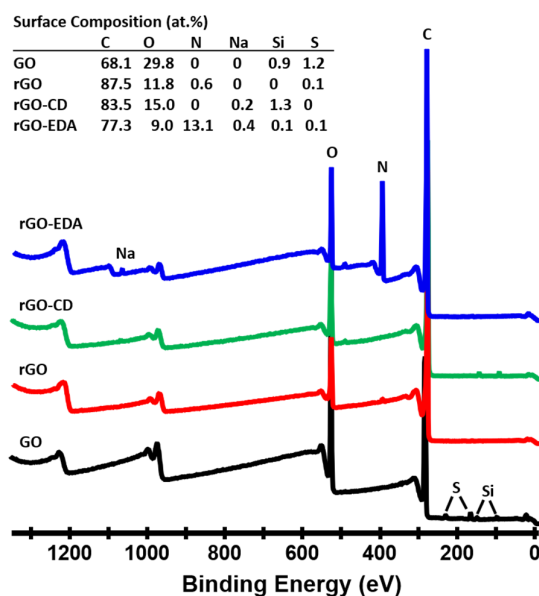


Figure S1. Survey spectra and surface composition of the GO and rGO, rGO-CD, and rGO-EDA aerogels.

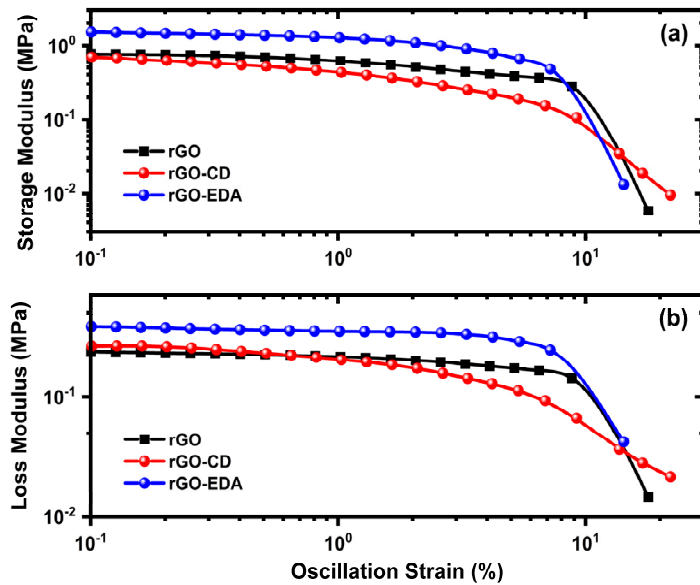


Figure S2. Rheological properties of the synthesized aerogels. (a) The storage and (b) loss modulus values according to oscillatory strain sweeps.

The Brunauer–Emmett–Teller (BET) measurements for the rGO and rGO-CD aerogels are shown in Figure S3. In the half pore width range from 30 to 80 Å, the derivative of the cumulative pore volume and the pore volume distributions were shifted to higher half pore width values for the cyclodextrin functionalized aerogel. The results are in good agreement with the small-angle neutron scattering measurements in Figure 5.

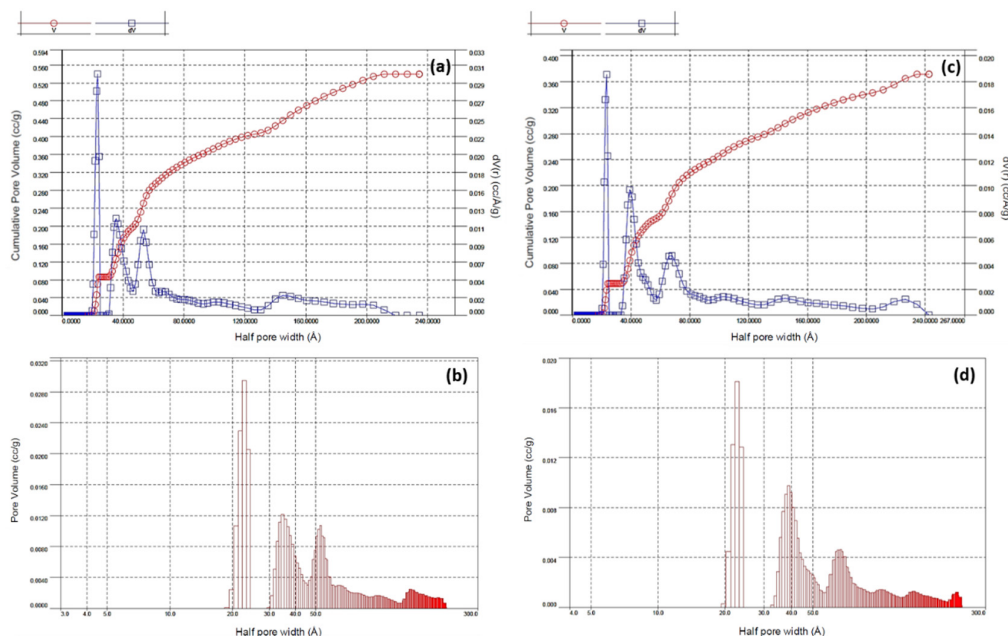


Figure S3. BET measurements for the (a,b) rGO and (c,d) rGO-CD aerogels.

To compare the surface composition of the aerogels with the surface composition of the graphite and graphene, XPS measurements (survey and core level spectra) of exfoliated graphite and graphene powder are shown in Figures S4-S6. The graphite was exfoliated in N-methyl-2-pyrrolidone (NMP) using a high-shear mixer with a rotor-stator configuration. For the XPS measurements the two powders were mounted on double-sided tape and loaded into the XPS analysis chamber through a vacuum load-lock. Initially, a wide energy survey scan was taken to verify the existence of known elements (C and O) and to determine if there were any unknown or contaminant species. The overall surface compositions for the exfoliated graphite and graphene are also presented in the inset tables in Figures S4-S6. The exfoliated graphite only showed C and O. In addition to C and O, the graphene also showed N and trace amounts of S and Si. Narrow energy range core level spectra were next acquired for C and O (and N for the graphene). For C 1s, the spectra in Figure S5 were fitted with six different peaks. For the sp^2 -type carbon three peaks (shown by the dotted black lines) were used. A single peak (shown by the solid black line) was used for the sp^3 -type carbon. C–O bonds were represented by a single peak (~286 eV) and C=O bonds were represented by a single peak (~287.5 eV). These peaks were constrained to keep the peak position within 0.5 eV of the expected positions and the full width at half maximum (FWHM) of the peaks were constrained to be about the same (within a few tenths of an eV). The C–O and C=O peak intensities were all similar to the corresponding peaks in the O 1s data (the O–C and O=C peaks are shown in the O 1s fitted spectrum). The inset table shows the atomic % for the various components. The same fitting scheme was used for the graphene in Figure S6, but with the addition of another peak in the C 1s spectrum for the C–N bonds. The C–N and C–O peaks overlap but can both be seen (C–O in red, C–N in dashed yellow). The table shows the atomic % for the various components.

The x-ray induced C KLL Auger spectra for the exfoliated graphite and graphene are shown in Figure S7. From the spectra, the D parameter was measured, which can be correlated to the amount of sp^2 -carbon. For a perfect graphite, the D parameter is 21 or higher. The D parameter for the exfoliated graphite is 21.2. The D parameter for the graphene is slightly lower because there is slightly more bonded carbon and sp^3 -type carbon.

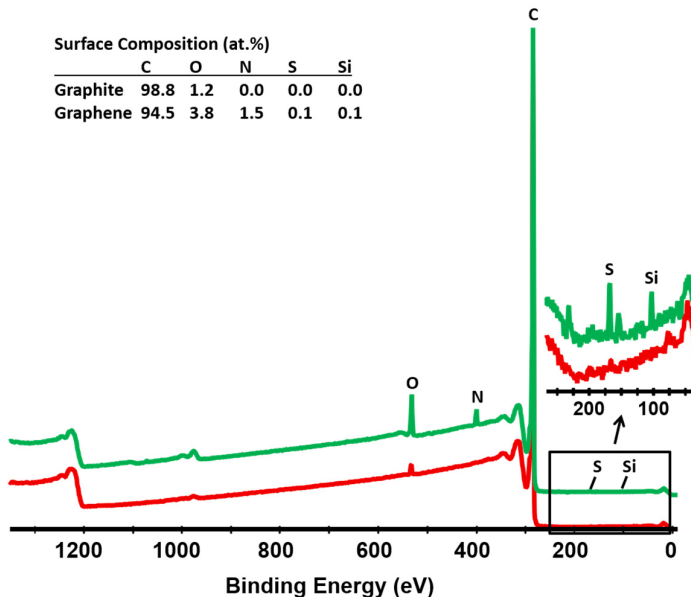


Figure S4. Survey spectra and surface composition of the exfoliated graphite and graphene.

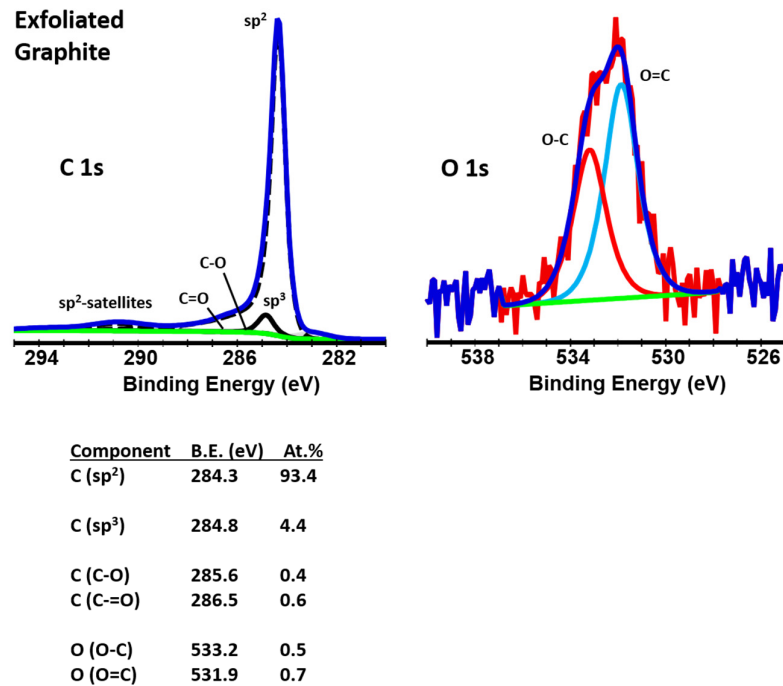


Figure S5. C 1s, and O 1s core level spectra, individual peak fitting and quantitative analysis of the surface functionalities for the exfoliate graphite.

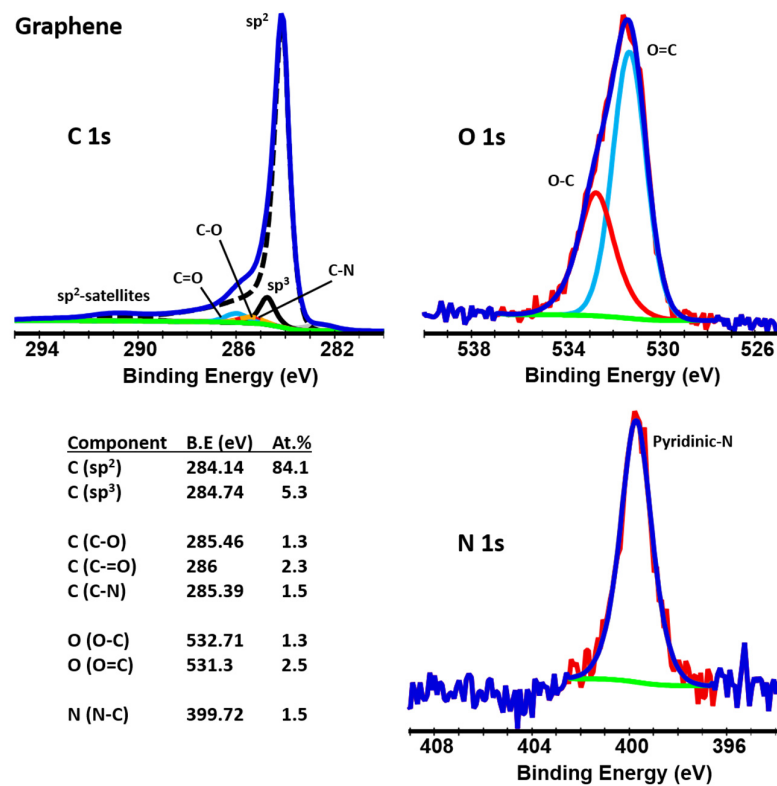


Figure S6. C 1s, O 1s, and N 1s core level spectra, individual peak fitting and quantitative analysis of the surface functionalities of graphene.

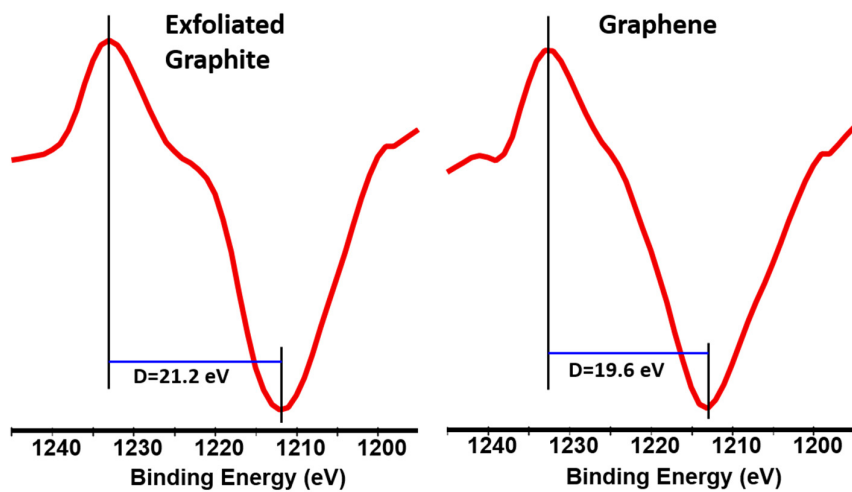


Figure S7. Auger spectra for the exfoliated graphite and graphene.

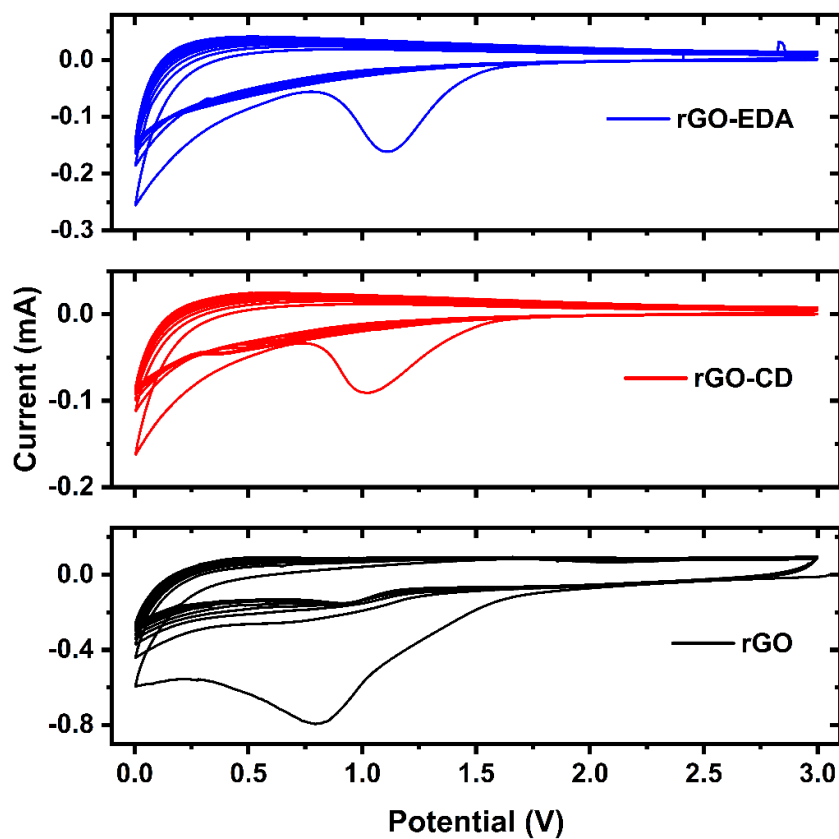


Figure S8. Cyclic voltammetry measurements of the rGO, rGO-CD, and rGO-EDA aerogels. The scan rate was 0.1 mV/s.

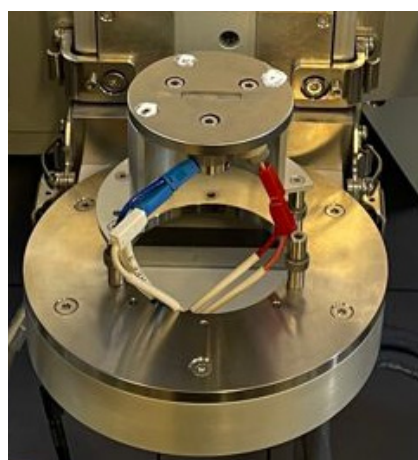


Figure S9. The electrochemical cell that was used to perform the operando XRD measurements.